Redox Biology 62 (2023) 102674

Contents lists available at ScienceDirect

Redox Biology

journal homepage: www.elsevier.com/locate/redox

ROS promote hyper-methylation of NDRG2 promoters in a DNMTS-dependent manner: Contributes to the progression of renal fibrosis

Yanfang Zhao [a], Xiaoting Fan [a], Qimeng Wang [a], Junhui Zhen [b], Xia Li [a], Ping Zhou [a], Yating Lang [c], Qinghao Sheng [c], Tingwei Zhang [c], Tongtong Huang [c], Yucheng Zhao [d], Zhimei Lv [a,*], Rong Wang [a,**]

[a] Department of Nephrology, Shandong Provincial Hospital, Shandong University, Jinan, Shandong, 250021, China
[b] Department of Pathology, School of Medicine, Shandong University, Jinan, Shandong, 250012, China
[c] Department of Nephrology, Shandong Provincial Hospital Affiliated to Shandong First Medical University, Jinan, Shandong, 250021, China
[d] College of Pharmacy, Jining Medical University, Shandong Province, Rizhao, 276826, China

ARTICLE INFO

Keywords:
NDRG2
DNA methylation
Reactive oxygen species
DNA methyltransferases
Renal fibrosis

ABSTRACT

Renal fibrosis is the common histopathological feature of chronic kidney diseases (CKD), and there is increasing evidence that epigenetic regulation is involved in the occurrence and progression of renal fibrosis. N-myc downstream-regulated gene 2 (NDRG2) is significantly down-regulated in renal fibrosis, the mechanism of which remains unclear. Previous studies have confirmed that the inhibition of NDRG2 expression in tumor cells is related to hyper-methylation, mainly regulated by DNA methyltransferases (DNMTS). Herein, we explored the expression of NDRG2 and its epigenetic regulatory mechanism in renal fibrosis. The results showed that the expression of NDRG2 was significantly inhibited in vivo and in vitro, while the overexpression of NDRG2 effectively alleviated renal fibrosis. Meanwhile, we found that the expression of DNMT1/3A/3B was significantly increased in hypoxia-induced HK2 cells and Unilateral Ureteral Obstruction (UUO) mice accompanied by hyper-methylation of the NDGR2 promoter. Methyltransferase inhibitor (5-AZA-dC) corrected the abnormal expression of DNMT1/3A/3B, reduced the methylation level of NDRG2 promoter and restored the expression of NDRG2. The upstream events that mediate changes in NDRG2 methylation were further explored. Reactive oxygen species (ROS) are important epigenetic regulators and have been shown to play a key role in renal injury due to various causes. Accordingly, we further explored whether ROS could induce DNA-epigenetic changes of the expression of NDRG2 and then participated in the development of renal fibrosis. Our results showed that mitochondria-targeted antioxidants (Mito-TEMPO) could reverse the epigenetic inhibition of NDRG2 in a DNMT-sensitive manner, showing strong ability of DNA demethylation, exhibiting epigenetic regulation and anti-fibrosis effects similar to 5-AZA-dC. More importantly, the anti-fibrotic effects of 5-AZA-dC and Mito-TEMPO were eliminated in HK2 cells with NDRG2 knockdown. These findings highlight that targeting ROS-mediated hyper-methylation of NDRG2 promoter is a potentially effective therapeutic strategy for renal fibrosis, which will provide new insights into the treatment of CKD.

1. Introduction

Chronic kidney disease (CKD) is an increasingly serious global public health problem, affecting as much as 8 to 18% of the world population [1], which brings a heavy burden to the society. Regardless of the underlying etiology of CKD which is characterized by progressive and irreversible loss of kidney, the main pathological feature is renal fibrosis [2]. In addition, renal fibrosis is the common ultimate pathway for progression to end-stage renal disease in almost all chronic and progressive kidney disease [3]. Despite recent studies have focused on investigating how the differential expression of key genes mediate the progression of renal fibrosis, the mechanisms of renal fibrosis have not

* Corresponding author. Department of Nephrology, Shandong Provincial Hospital, Shandong University; Shandong Provincial Hospital Affiliated to Shandong First Medical University, Jinan, Shandong, 250021, China.
** Corresponding author.
E-mail addresses: lvzhimei_sd@163.com (Z. Lv), Wangrong_sd@126.com (R. Wang).

https://doi.org/10.1016/j.redox.2023.102674
Received 14 February 2023; Received in revised form 9 March 2023; Accepted 14 March 2023
Available online 21 March 2023

been fully elucidated. Hence, understanding the underlying molecular mechanisms of renal fibrosis might reveal potential therapeutic modalities for CKD.

N-myc downstream-regulated gene 2 (NDRG2) is a cytoplasmic protein that belongs to the N-Myc downstream gene family [4]. It is widely expressed in a variety of normal tissues and has many biological functions, including cell growth and differentiation, stress responses and hormonal responses [5]. Previous studies have shown that NDRG2 is closely related to chronic fibrotic diseases. For instance, the expression of NDRG2 was reduced in fibrotic liver, while overexpression of NDRG2 could protect against liver fibrosis by suppressing the TGF-β1/Smad pathway and increasing the MMP2/TIMP2 ratio [5]. In addition, NDRG2 has been proved to be a potential regulator of renal fibrosis, and blocking the expression of NDRG2 could promote renal fibrosis by regulating the TGF-β/Smad3-mediated pro-fibrosis signaling pathway in HK2 cells [6]. All above findings indicate that NDRG2 may play a vital role in the pathogenesis of renal fibrosis. However, studies on the role and molecular mechanisms of NDRG2 in the development and progression of renal fibrosis are rather limited.

The NDRG2 promoter, which contains typical CpG islands, is regulated by DNA methylation. Several studies have shown that the hypermethylation of NDRG2 is related to the decreased expression of NDRG2 in a variety of tumors [7,8]. DNA methylation is the most studied epigenetic mechanism, and its role in renal fibrosis has been gradually explored in recent years. It refers to the regulatory process of adding a methyl group to CpG island cytosine residue under the mediation of DNMT1/3A/3B [9], which leads to gene inhibition and plays an important role in the regulation of gene expression [10]. Previous studies have shown that abnormal DNA hyper-methylation of multiple tumor suppressor genes is closely related to its transcriptional silencing in tumor cells, which is an important factor promoting the progression of cancer [11,12]. In addition, recent studies have found abnormal DNA methylation on the promoters of genes known to be associated with renal fibrosis in renal damage models [13–15], revealing the important role of DNA methylation in renal fibrosis and providing a potential therapeutic target for CKD. However, whether NDRG2 is an important regulator of epigenetic changes in renal fibrosis has not been confirmed.

Reactive oxygen species (ROS) are important epigenetic regulators. Studies have shown that higher levels of ROS promote the development of tumor through genetic and epigenetic mechanisms [16]. Specifically, ROS promote gene silencing by inducing abnormal hyper-methylation on promoters of tumor suppressor genes, leading to tumor invasion and metastasis [17,18]. ROS such as hydrogen peroxide (H2O2), superoxide ions (O2•−) and hydroxyl radicals (•OH) have been identified as one of the pathogenic factors of various diseases [19] and play a central role in signaling networks that regulate basic cellular processes [20]. Importantly, ROS are overproduced in the pathological state of CKD caused by various causes [21], which leads to the progression of CKD [22]. In addition, early intervention of excess ROS has been widely proven to prevent or delay the progression of CKD [23,24]. There is increasing evidence that oxidative stress induced by ROS can promote hyper-methylation of regional CpG islands and up-regulate DNA methylation levels by promoting the expression of DNMTS or forming new DNMT-containing complexes [25]. More importantly, ROS may contribute to the development and progression of renal fibrosis by promoting abnormal DNA methylation of target genes for renal fibrosis through increasing the expression of DNA methyltransferases [26–28]. However, whether ROS can induce epigenetic changes in NDRG2 to promote renal fibrosis and the key factors involved in this process remain unclear.

In this study, we analyzed the relationship between ROS and DNA methylation of NDRG2 in order to further explore the pathogenesis of renal fibrosis related to CKD. Our results revealed the key role of DNA hyper-methylation of NDRG2 in renal fibrosis and provided novel insights into potential prophylactic and therapeutic anti-renal fibrosis strategies.

2. Methods

2.1. Construction of animal models

All experimental procedures were performed in accordance with the guidelines of Laboratory Animal Care Committee of Shandong University (Shandong, China). Recombinant adeno-associated virus (AAV9-NDRG2) and adeno-associated virus negative control (AAV9-NC) were constructed by GENECHEM (Shanghai, China). C57BL/6 mice aged 6–8 weeks purchased from Shandong Animal Experimental Center were randomly allocated into four groups: (1) Control group: Sham operation (n = 6); (2) UUO group: unilateral ureteral obstruction operation (n = 6); (3) AAV9-NC + UUO group: AAV9-NC administered before UUO operation (n = 6); (4) AAV9-NDRG2+UUO group: AAV9-NDRG2 administered before UUO operation (n = 6). The model of UUO was established according to the method described in previous literatures [29]. Briefly, the left ureter was exposed after anesthesia in all mice and then the ureter was ligated with silk sutures for 14 days in the experimental group, while no treatment was done in the control group. Mice in the AAV9-NDRG2 and AAV9-NC group received tail vein injection of AAV9-NC or AAV9-NDRG2, with a dose of 100 μl phosphate buffer saline (PBS) containing 2 × 10^11 vector genome (vg) per mouse. Mice in control group were injected with the same volume of PBS. After 3 weeks, UUO model was carried out. The ability of AAV9 viral vector injected through tail veins to transduce the kidneys of C57BL/6 mice was determined using frozen kidney tissue sections (Supplementary Fig. 2). In addition, the results of Western blotting showed that NDRG2-overexpressed mice were successfully constructed (Supplementary Fig. 2).

For some experiments, mice were randomly assigned to one of three groups: (1) Control group (n = 6) ; (2) UUO group (n = 6); (3) 5-AZA-dC + UUO group: 5-AZA-dC administered before UUO operation (n = 6) or (3) Mito-TEMPO + UUO group: Mito-TEMPO administered before UUO operation (n = 6). Mice treated with 5-AZA-dC were intraperitoneally injected with 5-AZA-dC (0.35 mg/kg, A3656, Sigma-Aldrich, USA) every other day from day 1 before surgery to the day of euthanasia. The same injection regimen was followed for Mito-TEMPO (1 mg/kg, SML0737, Sigma-Aldrich, USA) treated mice. Mice in control group were injected with the same volume of PBS. For some experiments, C57BL/6 mice aged 6–8 weeks were randomly allocated into five groups: (1) Control group (n = 6); (2) UUO group (n = 6) (3) AAV9-NC + UUO group (n = 6); (4) AAV9-NDRG2+UUO group (n = 6); (5) AAV9-NDRG2+5-AZA-dC + UUO group: Mice overexpressing NDRG2 were injected with 5-AZA-dC before UUO operation, using the same dosage and method as previously described (n = 6).

2.2. Histology and immunohistochemistry

The kidneys of mice were fixed with 10% formalin, embedded in paraffin, and cut into 4 μm sagittal sections. Hematoxylin-eosin staining (H&E), Periodic Acid-Schiff staining (PAS) and Masson-trichrome staining were performed according to the manufacturer's instructions. For immunohistochemistry, the sections were incubated with primary antibodies against NDRG2 (1:100, Abcam, UK), E-cadherin (1:100, Abcam), Fibronectin (1:200, Proteintech, USA), Collagen-I (1:100, Proteintech, USA), and α-SMA (1:100, Abcam), DNMT1 (1:200, Abcam), DNMT3A (1:200, Abcam), DNMT3B (1:200, Proteintech).

2.3. Cell culture

Human renal tubular epithelial cells (HK2) were seeded in 6-well plates at a density of 5000 cells/cm^2 and grown in 1640 medium (Gibco, USA) containing 10% fetal bovine serum (FBS) and 1% penicillin-streptomycin (Solarbio, Beijing, China). For hypoxia experiment, cells were exposed to 1% O_2, 5% CO_2 at 37 °C in the hypoxic chamber (Thermo Fisher, USA). For the treatment with

methyltransferase inhibitors, cells were pretreated with 5-AZA-dC (1 μM, Sigma-Aldrich) 1 h before exposed to hypoxia. For the treatment with ROS inhibitors, cells were pretreated with Mito-TEMPO (10 μM, Sigma-Aldrich) 2 h before exposed to hypoxia. For the treatment with glutathione precursors, cells were pretreated with GSHee (2 mM, Sigma-Aldrich) or NAC (5 mM, MedChemExpress) 1 h before exposed to hypoxia.

2.4. Lentiviral vector transduction

Lentivirus vectors encoding NDRG2 (NDRG2 vector), an empty lentiviral vector (NULL vector), lentivirus interference vector against NDRG2 (NDRG2 shRNA) and control lentiviral vector (scramble vector) were purchase from Cyagen (Guangzhou, China). Lentivirus transfections of HK2 were performed according to the manufacturer's instructions. Transfection efficiencies were assessed by RT-PCR and Western blotting.

2.5. Western blotting

Protein was extracted from HK2 cells and mice kidney by Lysis buffer supplemented with 10% protease inhibitors. Equal amounts of protein samples from each group were loaded on 10% SDS-PAGE gel in order and then transferred onto poly vinylidene fluoride (PVDF) membrane. After blocking in 5% skim milk for 1 h, the membranes were incubated at 4 °C overnight with primary antibodies against GAPDH (1:1000, Proteintech), NDRG2 (1:1000, Abcam), E-cadherin (1:1000, Cell Signaling Technology,USA), N-cadherin (1:2000, Abcam), Vimentin (1:2000, Abcam), α-SMA (1:2000,Abcam), Collagen-I (1:1000, Proteintech), Fibronectin (1:2000, Proteintech), DNMT1 (1:1000, Abcam), DNMT3A (1:1000, Abcam), and DNMT3B (1:1000, Proteintech). The next day, the membranes were incubated with different secondary antibodies: horseradish peroxidase-conjugated goat anti-rabbit IgG (1:5000, Abcam) or horseradish peroxidase-conjugated goat anti-mouse IgG (1:5000, Abcam) for 1 h. Finally, the results were analysis using ECL reagent (Millipore, USA) and Amersham Imager 600 (GE, USA). The protein content was analyzed with Image J software.

2.6. Quantitative real-time PCR analysis

Total RNAs were extracted from HK2 cells and mice kidney using Trizol reagent (Takara, Japan) according to the manufacturer's instructions. Reverse transcription kits (Takara, Japan) were used to reverse transcribe RNA into cDNA according to the manufacturer's instructions. SYBR Green PCR kits (Takara, Japan) were used for Real-time PCR and the primers are listed in Supplementary Table 1.

2.7. Immunofluorescence analysis

The HK-2 cells were cultured on cover-slips and treated accordingly. Then, the cells were washed and fixed with formaldehyde for 15 min. Cells were selectively treated with or without 0.5% Triton X-100 for 5 min, depending on the location of protein expression. Next, cells were incubated with blocking medium (PBS containing 5% bovine serum albumin) for 1 h at 37 °C, then incubated at 4 °C overnight with primary antibodies against E-cadherin (1:100, Cell Signaling Technology), Vimentin (1:200, Abcam), α-SMA (1:100, Abcam), DNMT1 (1:100, Abcam), DNMT3A (1:100, Abcam), DNMT3B (1:100, Proteintech). Subsequently, the cells were washed and incubated at room temperature with Alexa Fluor® 594-conjugated goat anti-rabbit IgG (1:200, Abcam) for 1 h. The nuclei were stained with 4′, 6-diamidino-2-phenylindole (DAPI, Sigma-Aldrich). Then the cells were imaged on fluorescence Microscope (Leica Microsystems GmbH, Germany).

2.8. Mito SOX Red mitochondrial superoxide

Mitochondrial ROS activity was analyzed using the MitoSOX Red Mitochondrial Superoxide Indicator (YEASEN Biotech, China). The HK-2 cells were cultured on cover-slips and treated accordingly. Cells were washed and fixed with formaldehyde for 15 min, and then were incubated in MitoSOX (5 μM) in Hank's balanced salt solution (HBSS) for 30 min at 37 °C. The nuclei were stained with DAPI. Images were taken by fluorescence Microscope (Leica Microsystems GmbH).

2.9. Methylation-specific PCR (MSP) and bisulfite-sequencing PCR (BSP)

The prediction of CpG islands in the NDRG2 gene and the designing of MSP primers and BSP primers were performed with the online MethPrimer software (http://www.urogene.org/methprimer). The predicted CpG islands of the NDRG2 gene in human and the locations of MSP primers are plotted in Fig. 3J. The predicted CpG islands of the NDRG2 gene in mouse and the locations of BSP primers are plotted in Fig. 5C. The primer sequences for MSP and BSP were listed in Supplementary Tables 2 and 3. The genomic DNA was extracted from HK2 cells and mouse kidney tissues (Fast Pure Blood/Cell/Tissue/Bacteria DNA Isolation Mini Kit, Vazyme Biotech). For MSP analyses, human genomic DNA was modified by bisulfate treatment (EZ DNA Methylation-Gold Kit, Zymo Research). The IQ5 real-time PCR detection system (Bio-Rad, Hercules, CA) was used for MSP analysis, according to the manufacturer's instruction. The PCR products were visualized by ethidium bromide staining in 2% agarose gels, and the densitometric intensity corresponding to each band was quantified, and then the ratio of methylation or unmethylation band intensity over total PCR products was calculated. PCR amplification profiles were essentially as following: initial denatured at 95 °C for 8min, annealing and extension: (95 °C × 1min/60 °C × 30 s/72 °C × 30 s) for a total of 40 cycles and final extension at 72 °C for 10min.

Three randomly selected mice from control, UUO, 5-AZA + UUO or Mito-TEMPO + UUO group were subjected for BSP assay. The PCR products were separated by electrophoresis, and the target DNA fragments were purified and cloned into pGEM T Easy Vector (A1360; Promega). Eight clones from each sample were picked for sequencing analysis.

2.10. Chromatin immunoprecipitation and quantitative PCR

DNMT1 (Abclonal, USA), DNMT3A (Abclonal), DNMT3B (Proteintech) antibodies and normal rabbit IgG (1 μg) were used for chromatin immunoprecipitation (ChIP) assays, which were performed using a ChIP assay kit (Beyotime Biotechnology, China), according to the manufacturer's protocol. DNA recovered and purified from the immune-precipitated complexes was subjected to quantitative PCR (qPCR).

2.11. Dual-luciferase system

Dual-luciferase reporter was obtained using a Dual-luciferase reporter assay system kit (Promega, USA). Briefly, HK2 cells were co-transfected with human NDRG2 promoter reporter plasmid (pGL3-NDRG2-Luc) plus the renilla luciferase reporter plasmid (pRL-TK) with Lipofectamine 2000 (Invitrogen, USA) following the manufacturer's instructions. The transfected cells were cultured in hypoxia condition for 48 h in presence or absence of 5-AZA-dC or Mito-TEMPO before further analysis. The reporter luciferase activities were determined as the results of reporter activities divided by renilla activities and normalized. All the transfection experiments were performed in triplicate and repeated at least three times independently.

2.12. Flow cytometry

For apoptosis analysis, HK2 cells were treated accordingly and

processed according to the PE Annexin V Apoptosis Detection Kit I (BD, San Jose, CA, USA) and analyzed by a FACS can flow cytometer.

2.13. TUNEL

The apoptotic cells in kidney tissue sections were detected using a TUNEL apoptosis detection kit (Elabscience Biotechnology Co. Ltd, China) according to the instructions provided by the manufacture. Briefly, paraffin-embedded sections were treated with fresh diluted proteinase K for 30 min at 37 °C after deparaffinage and rehydration. TdT enzyme reaction mixture was applied to each slide at 37 °C for 2 h. At last, the slides were reacted with DAPI solution for 10 min at room temperature. Controls for this procedure included a slide where the TdT enzyme was omitted and another where the slide was pretreated with DNAse I before the normal TUNEL procedure. Images were taken by fluorescence Microscope (Leica Microsystems GmbH). Positive cells were counted using Image J software.

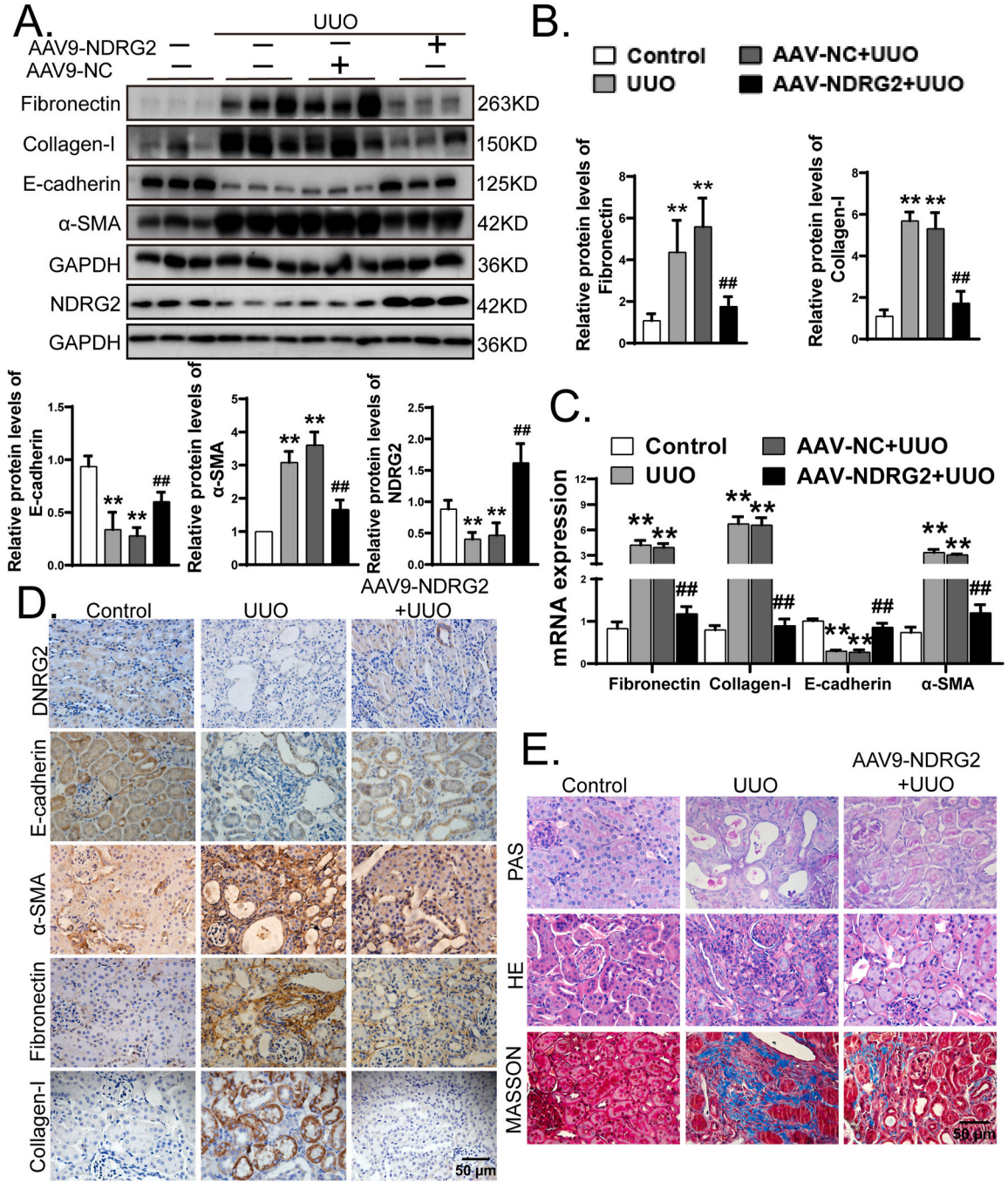

Fig. 1. Overexpression of NDRG2 prevented renal fibrosis in UUO mice. Mice in the AAV9-NDRG2 and AAV9-NC group were received tail vein injection of AAV9-NC or AAV9-NDRG2, following the method described earlier. Then, C57BL/6 mice were subjected to ligation of left urteter (UUO) or sham operation (control). The mice were sacrificed 14 days after surgery. (A) Protein expressions levels of Fibronectin, Collagen-I, E-cadherin, α-SMA and NDRG2 from control, UUO, AAV9-NC + UUO and AAV9-NDRG2+UUO mice assayed by Western blotting (3 samples from each group). (B) Quantification of (A). (C) Gene expressions levels of Fibronectin, Collagen-I, E-cadherin, α-SMA assayed by Real-time PCR. (D) Representative renal immunohistochemical staining of NDRG2, E-cadherin, α-SMA, Fibronectin and Collagen-I from experimental mice as above. (E) Representative images of H&E, PAS and Masson's trichrome staining in control group, UUO group and AAV9-NDRG2+UUO group. The statistics were based on at least three independent experiments. $^{**}p < 0.01$ versus control, $^{\#\#}p < 0.01$ versus UUO by one-way ANOVA.

2.14. Statistical analysis

GraphPad Prism 8 was used to analyze experimental data. The results were shown as the mean ± standard deviation (SD). Statistical significance between two groups was determined by Student t-test, while significance among multiple groups was determined by one-way ANOVA. $P < 0.05$ indicated a statistically significant difference. All experiments were repeated at least three times unless otherwise stated.

3. Results

3.1. Overexpression of NDRG2 prevented renal fibrosis in UUO mice

To gain insights into the role of NDRG2 in CKD, we established mice model of CKD by UUO. Two weeks after ligation of ureter, the left kidneys of mice were collected for histological analysis. The expression levels of epithelial marker E-cadherin and mesenchymal markers including Fibronectin, Collagen-I, α-SMA, N-cadherin and Vimentin were detected by Western blotting, PCR assays and immunohistochemistry. Renal damage and fibrosis were evaluated using H&E, PAS and Masson trichrome staining. We found that compared with control group, kidneys from UUO mice displayed marked reduction of epithelial marker E-cadherin. Inversely, UUO mice displayed induction of Vimentin, α-SMA, Collagen-I and Fibronectin (Supplementary Fig. 1A-C, E). Moreover, histological examination of the kidneys in UUO mice exhibited severe tubular dilation and atrophy, intratubular cast formation, inflammatory cell infiltration as well as collagen deposition in tubular interstitial area (Supplementary Fig. 1D). All above indicated that renal fibrosis model was successfully established. To clarify the role of NDRG2 in UUO, the expression levels of NDRG2 in kidneys from control group and UUO group were detected. We found that the mRNA and protein levels of NDRG2 was moderately decreased in UUO mice (Supplementary Fig. 1 A-C, E), which indicating a potential role for NDRG2 in regulating UUO-induced renal fibrosis.

To provide more direct evidence for the role of NDRG2 in the progression of renal fibrosis in UUO mice, we constructed mice overexpressing NDRG2 by injecting adeno-associated virus containing NDRG2 gene (Supplementary Fig. 2), which is consistent with the studies of Ma et al. [30], Wang et al. [31], and Zhang et al. [32]. Then the mice were subjected to sham-operation or ligation of the left ureter, and the left kidneys were collected 14 days after surgery. Considering that NDRG2 may affect apoptosis, the effect of overexpression of NDRG2 on apoptosis was detected by TUNEL assay. As shown in Supplementary Fig. 3, the proportion of TUNEL positive cells increased slightly in the NDRG2 overexpression group, but there was no statistical difference from the control group. We found that following UUO, AAV-NDRG2 treatment mitigated abnormal expression of Fibronectin, Collagen-I, α-SMA, and E-cadherin (Fig. 1A–C). In addition, immunohistochemical staining indicated that in UUO mice, AAV9-NDRG2 treatment reversed the decrease of E-cadherin and NDRG2 and the increase of mesenchymal markers (α-SMA, Collagen-I and Fibronectin) (Fig. 1D). Furthermore, mice overexpressing NDRG2 showed more minor histopathological damage, structural damage, and renal fibrosis severity than AAV-NC mice (Fig. 1E). Taken together, these results indicated that inhibition of NDRG2 deficiency could alleviate renal fibrosis under pathologic conditions of UUO.

3.2. NDRG2 was crucial for the normalization of fibrotic protein expression in HK2 cells under hypoxia conditions

In order to further verify the role of NDRG2 in the pathogenesis of renal fibrosis, we examined the expression of NDRG2 and renal fibrosis-related proteins in HK2 cells. Previous studies have reported that hypoxia is an early event of obstruction-induced renal fibrosis [29]. Corresponding to the in vivo experiments, HK2 cells were cultured in a hypoxic environment to simulate the micro-environment of HK2 cells in patients with CKD. HK2 cells were cultured in hypoxia chamber (1% O_2) for different periods of time (for 24 h and 48 h) to observe whether hypoxia increased cell fibrotic protein expression and the cells cultured under normoxia served as control. Remarkably, the expression level of NDRG2 and E-cadherin were significantly decreased in HK2 cells after 48h of hypoxia, whereas the expression levels of N-cadherin, Vimentin and α-SMA were significantly increased (Fig. 2A–C), which was in line with the results of in vivo experiments. To further determine the role of NDRG2 in the progression of cells fibrotic response, we investigated the effects of NDRG2 knockdown on basal levels of several key proteins in HK2 cells. Firstly, we constructed a lentiviral vector for human NDRG2 that could specifically overexpress or knockdown NDRG2 after transfection of HK2 cells (Supplementary Fig. 4A-C and 5A–C). We found that NDRG2 knockdown led to an increased basal expression of N-cadherin and Vimentin, while a decreased basal expression of E-cadherin compared to HK-2 cells treated with Scramble vector (Supplementary Figs. 5A–C). These results suggested that NDRG2 controlled the basal expressions of these proteins. Next, we tried to explore whether the same effect could be achieved after hypoxia stimulation with HK2 cells. HK2 cells with normal expression, over-expression and low expression of NDRG2 were cultured in hypoxia condition (1% O_2) for 48 h and the cells cultured under normoxia served as control. We found that NDRG2 knockdown led to more significantly increased expression levels of Fibronectin, Collagen-I, N-cadherin, Vimentin and α-SMA significantly decreased expression levels of E-cadherin under hypoxia exposure (Supplementary Figs. 5D–F). Conversely, overexpression of NDRG2 successfully returned the abnormal levels of E-cadherin and mesenchymal markers to control levels (Fig. 2D–F). Consistently, the results of immunofluorescence indicated that the expression of E-cadherin, α-SMA and Vimentin in HK2 under hypoxia exposure was markedly reversed by NDRG2 vector (Fig. 2G–I). Taken together, these data strongly suggested that NDRG2 was a key factor in the resistance to fibrotic responses in HK2 cells under hypoxia conditions.

3.3. NDRG2 was regulated epigenetically via promoter methylation in hypoxia-induced HK2 cells

Human NDRG2 promoters contain typical CpG islands and NDRG2 promoter hyper-methylation has been reported in a variety of tumors [33,34]. We speculated that hypoxia-associated NDRG2 loss might involve aberrant epigenetic DNA methylation. Because DNA hyper-methylation correlates with a gain of function of DNMT, we measured the expression of DNA methylation-related proteins, including DNMT1, DNMT3A and DNMT3B. Our results showed that HK2 cells in hypoxia group displayed marked increase of DNMT1/3A/3B (Fig. 3A and B), which indicated hypoxia induced abnormal DNA hyper-methylation in HK2 cells. In addition, HK2 cells were pretreated with different concentrations of 5-AZA-dC, a DNMTS inhibitor, which is reported to inhibit the activity of DNMTS. We found that with the increase of concentration of 5-AZA-dC, the expression level of DNMT1/3A/3B gradually decreased, while the expression level of NDRG2 gradually increased. In addition, the use of 5-AZA-dC could effectively inhibit fibrotic protein expression in hypoxia-induced renal tubular epithelial cell (Fig. 3A and B). We found that when the concentration of 5-AZA-dC was 1 μM, the abnormal expression of DNMT1/3A/3B and the inhibition of NDRG2 induced by hypoxia were significantly reversed without causing HK2 cells apoptosis (Supplementary Figs. 6A and B). Therefore, this concentration group was used in the follow-up experiment. In addition, the results of PCR (Fig. 3C) and immunofluorescence staining (Fig. 3D–I) showed that the abnormal expression of DNMT1/3A/3B, Fibronectin, E-cadherin, Vimentin, and α-SMA was significantly reversed when the concentration of 5-AZA-dC was 1 μM. To gain additional insight into the possible involvement of DNA methylation alteration in NDRG2 reduction in hypoxia-induced HK2 cells, we performed MSP on a selected CpG-rich area (as picked by MethPrimer software) on human NDRG2 promoter and

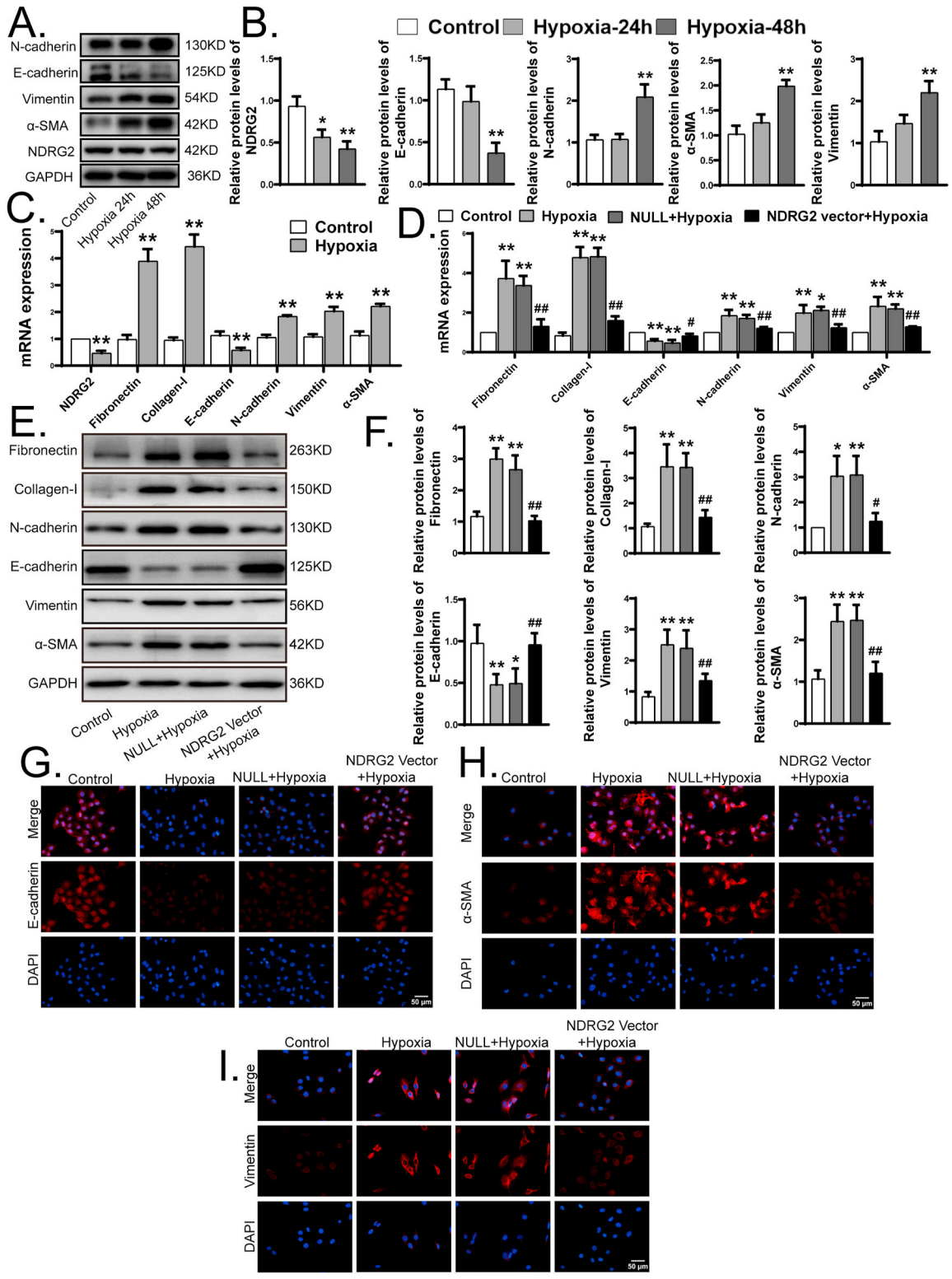

Fig. 2. NDRG2 was crucial for the normalization of fibrotic protein expression in HK2 cells under hypoxia conditions. (A) Western blotting assay for the expression of NDRG2, E-cadherin, N-cadherin, Vimentin and α-SMA in HK2 cells cultured at 1% oxygen concentration for 24, 48 h. (B) Quantification of (A). (C) Real-time PCR analysis in HK2 cells. (D) Real-time PCR analysis in HK2 cells transfected with NULL vector, NDRG2 vector and then cultured in normxia or hypoxia conditions for 48h. (E) Western blotting assay of protein expression levels. (F) Quantification of (E). (G–I) Representative immunofluorescence images of E-cadherin, Vimentin and α-SMA in HK2 cells. The statistics were based on at least three independent experiments. *$p < 0.05$, **$p < 0.01$ versus control; $^{\#}p < 0.05$, $^{\#\#}p < 0.01$ versus NULL + hypoxia by one-way ANOVA.

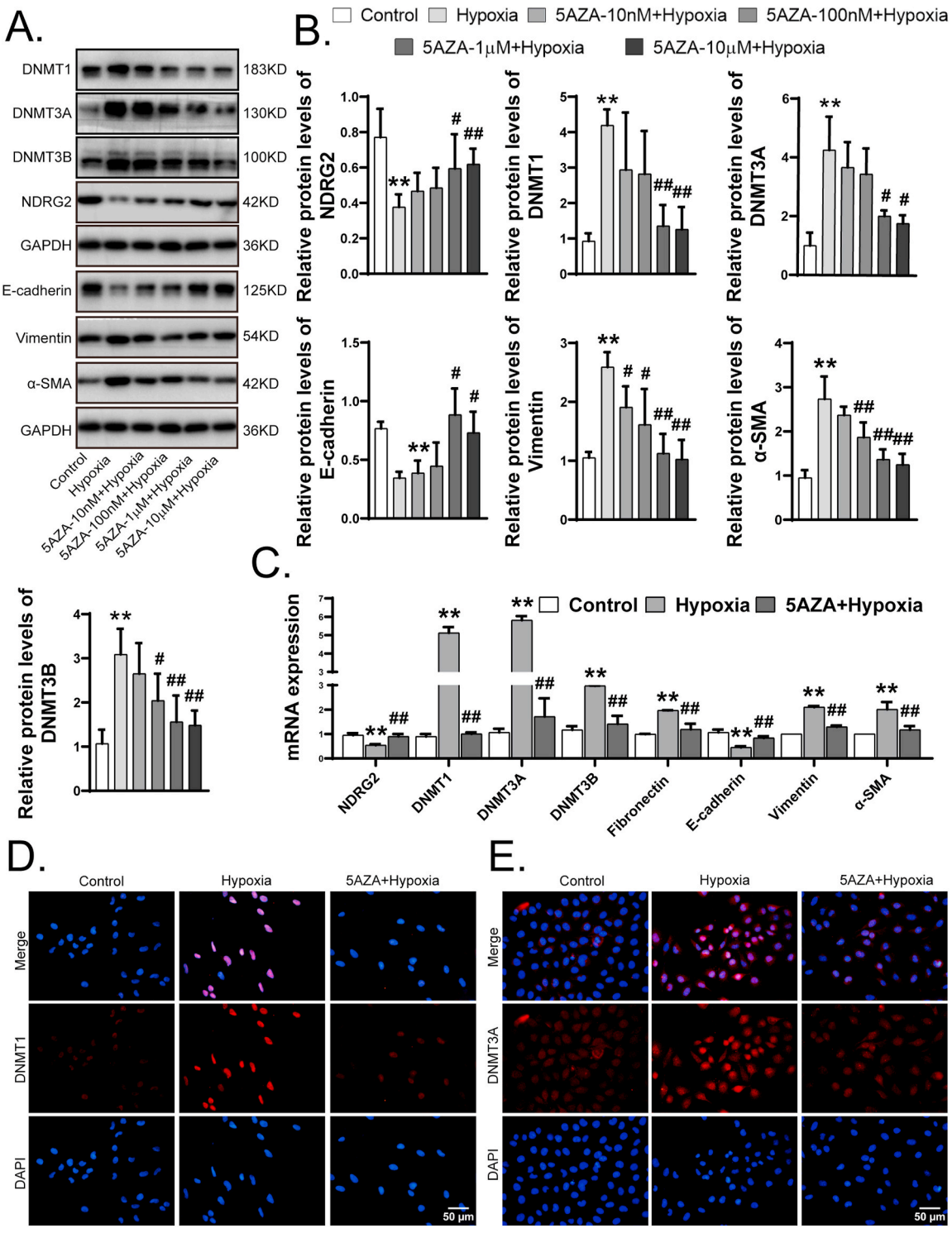

Fig. 3. NDRG2 was regulated epigenetically via promoter methylation in hypoxia-induced HK2 cells. (A) Western blotting assay for the expression of DNMT1, DNMT3A, DNMT3B, NDRG2, E-cadherin, Vimentin and α-SMA in HK2 cells pretreated with 5-AZA-dC at different concentrations (10 nM, 100 nM, 1 μM, and 10 μM) for 1 h and cultured in normxia or hypoxia conditions for 48 h. (B) Quantification of (A). (C) Real-time PCR analysis in HK2 cells. (D–I) Representative immunofluorescence images of DNMT1, DNMT3A, DNMT3B, E-cadherin, Vimentin and α-SMA. (J) Schematic diagram of human NDRG2 promoter. The CpG island is in gray. The relative locations of methylation-specific polymerase chain reaction (MSP) primers are indicated. (K) MSP analysis of NDRG2 promoter methylation in HK2 cells. (L) Quantifications for (K). (M) Luciferase assay. A Human NDRG2 promoter reporter plasmid plus a renilla luciferase control were co-transfected into HK2 cells and the cells were cultured in normxia or hypoxia conditions in presence or absence 5-AZA-dC for the following 48h. The cell lysates were assayed for luciferase activities, which were normalized with renilla activities. (N) ChIP-qPCR using primer sets specific for NDRG2 promoter. ChIP products using antibodies against DNMT1, DNMT3A and DNMT3B were analyzed by qPCR. The statistics were based on at least three independent experiments. *$p < 0.05$, **$p < 0.01$ versus control, $^{\#}p < 0.05$, $^{\#\#}p < 0.01$ versus hypoxia by one-way ANOVA.

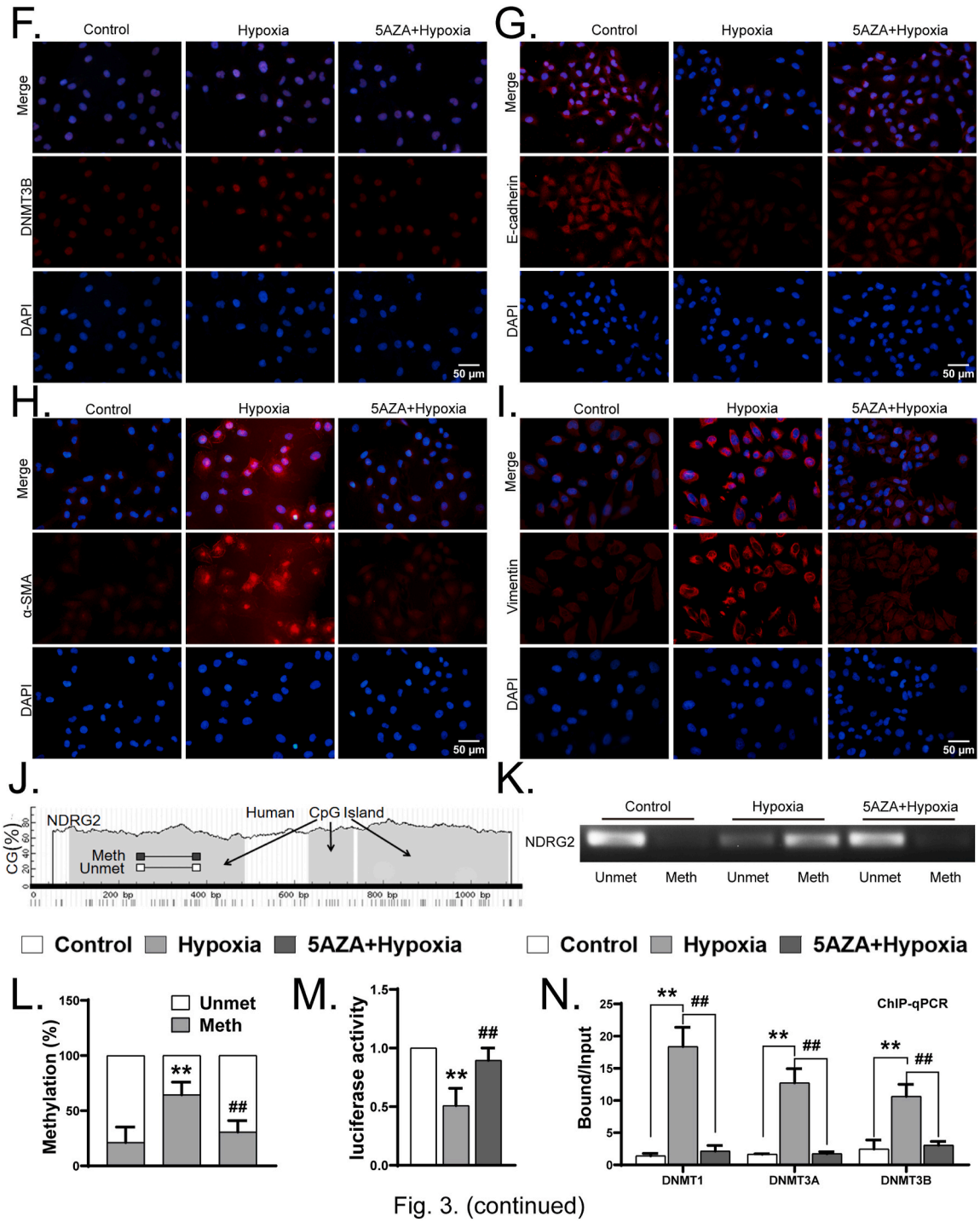

Fig. 3. (continued)

Fig. 3. (*continued*).

semi-quantitatively analyzed the PCR products. MSP revealed that NDRG2 promoter displayed low basal methylation in control group (about 21%), however, HK2 cells in hypoxia group exhibited increased methylation up to 65%. On the contrary, the use of 5-AZA-dC inhibited this hyper-methylation to 30% (Fig. 3J–L). Collectively, these results suggested that hypoxia-associated NDRG2 repression was due to NDRG2 promoter hyper-methylation, which was likely associated with aberrant DNMTS expression. In addition, the dual-luciferase reporter gene assay verified that hypoxia decreased the transcription of NDRG2 promoter reporter that contained partial CpG islands, which was inhibited by 5-AZA-dC (Fig. 3M), suggesting that abnormal changes in DNMTS expression affected the transcription of NDRG2 in response to hypoxia-induced cellular fibrotic response. To further clarify the role of DNMTS in NDRG2 promoter hyper-methylation in HK2 cells under hypoxia exposure, we used ChIP-qPCR to analyze whether DNMT1, DNMT3A and DNMT3B could bind to the NDRG2 promoter region of HK2 cells and the effect of hypoxia on their binding ability with or without 5-AZA-dC. We found that all of three DNMTS strongly bind to the NDRG2 promoter region in hypoxia condition. On the contrary, 5-AZA-dC treatment significantly reduced the binding force between them (Fig. 3N). All together, these results clarified that hypoxia suppressed NDRG2 likely through inducing aberrant DNMTS-associated

NDRG2 promoter hyper-methylation in HK2 cells.

3.4. NDRG2 was crucial for the anti-fibrotic effects mediated by 5-AZA-dC in hypoxia-induced HK2 cells

We hypothesized that if NDRG2 retention was critical for anti-fibrotic effects mediated by 5-AZA-dC in hypoxia-induced HK2 cells, and that the deletion of NDRG2 would eliminate this effect. To demonstrate our suppose, HK2 cells with NDRG2 knockdown were treated with 5-AZA-dC. We found that the anti-fibrotic activities of 5-AZA-dC were largely abolished when NDRG2 was knocked down (Fig. 4A–C). Overall, these results strongly revealed that NDRG2 was required for the anti-fibrotic effects mediated by 5-AZA-dC in HK2 cells under hypoxic environment.

3.5. 5-AZA-dC alleviated NDRG2 promoter hyper-methylation and UUO-associated renal fibrosis

To gain additional insight into the possible involvement of DNA methylation alteration in NDRG2 reduction in UUO kidney, we examined the DNMTS expression by immunohistochemistry. We found that kidneys of UUO mouse displayed dramatic increases of DNMT1, DNMT3A and DNMT3B (Supplementary Figs. 7A–C), which were in line with the in vitro experiment. Then we further examined the potential role of 5-AZA-dC on UUO-induced NDRG2 reduction and kidney fibrosis. Mice were injected with 5-AZA-dC (120 mg/kg) intraperitoneally every other day from day 1 before surgery and the mice were sacrificed at 14 days after UUO. We found that 5-AZA-dC significantly mitigated abnormal expression of DNMTS (Fig. 5A and B). To further explore the potential epigenetic mechanisms of aberrant DNA methylation that might account for NDRG2 suppression, we analyzed the NDRG2 promoter by the online software MethPrimer (http://www.urogene.org/methprimer). As show in Fig. 5C, mouse NDRG2 gene promoter is characterized by typical CpG islands (gray areas). Subsequently, BSP assay, the gold standard of methylation analysis, was performed on mouse kidney tissue. The results of BSP assay revealed that UUO kidney showed a significant increase of NDRG2 promoter methylation from 0.83 ± 0.72% to 7.92 ± 2.89% ($P < 0.01$), but 5-AZA-dC treatment reduced the level to 1.67 ± 0.72% ($P < 0.01$, Fig. 5D and E). Collectively, these results suggested that UUO-associated NDRG2 repression was due to NDRG2 promoter hyper-methylation, and 5-AZA-dC might inhibit NDRG2 suppression by blocking DNMTS aberrations and subsequent NDRG2 promoter hyper-methylation, which was consistent with in vitro results. In addition, histologic examinations showed that kidneys of UUO mouse displayed tubular atrophy, increased cell density, intratubular cast formation as well as collagen deposition in tubular interstitial area. However, 5-AZA-dC treatment effectively reduced these pathologic changes (Fig. 5F). Furthermore, our results showed that 5-AZA-dC mitigated abnormal expression of NDRG2 and fibrosis-related proteins induced by UUO (Fig. 5G–I). To further investigate whether the anti-renal fibrosis effect of 5-AZA-dC was dependent on NDRG2, mice overexpressing NDRG2 were pretreated with 5-AZA-dC the day before UUO surgery. As shown in Fig. 5J and K, there was no further remission of renal fibrosis in mice overexpressing NDRG2 after exposure to 5-AZA-dC. Together, these findings demonstrated that 5-AZA-dC could restore the expression of NDRG2 by

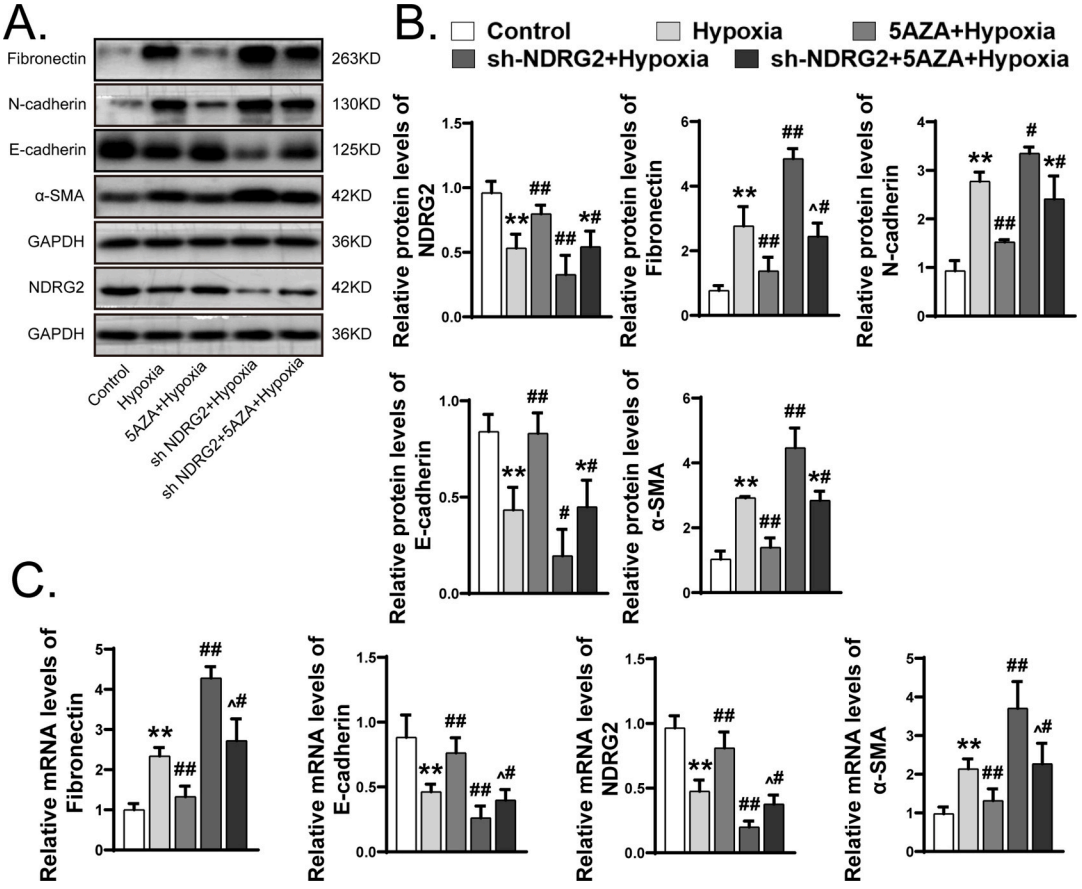

Fig. 4. NDRG2 was crucial for the anti-fibrotic effects mediated by 5-AZA-dC in hypoxia-induced HK2 cells. (A) Western blotting assay for the protein expression of NDRG2, Fibronectin, N-cadherin, E-cadherin and α-SMA in HK2 cells transfected with NDRG2 shRNA or Scramble shRNA cultured in hypoxia or normoxia for 48h with or without 5-AZA-dC. (B) Quantification of (A). (C) Real-time PCR analysis in HK2 cells. The statistics were based on at least three independent experiments. *p < 0.05, **p < 0.01 versus control; #p < 0.05, ##p < 0.01 versus hypoxia; ^#p < 0.05, *#p < 0.01 versus shNDRG2+hypoxia by one-way ANOVA.

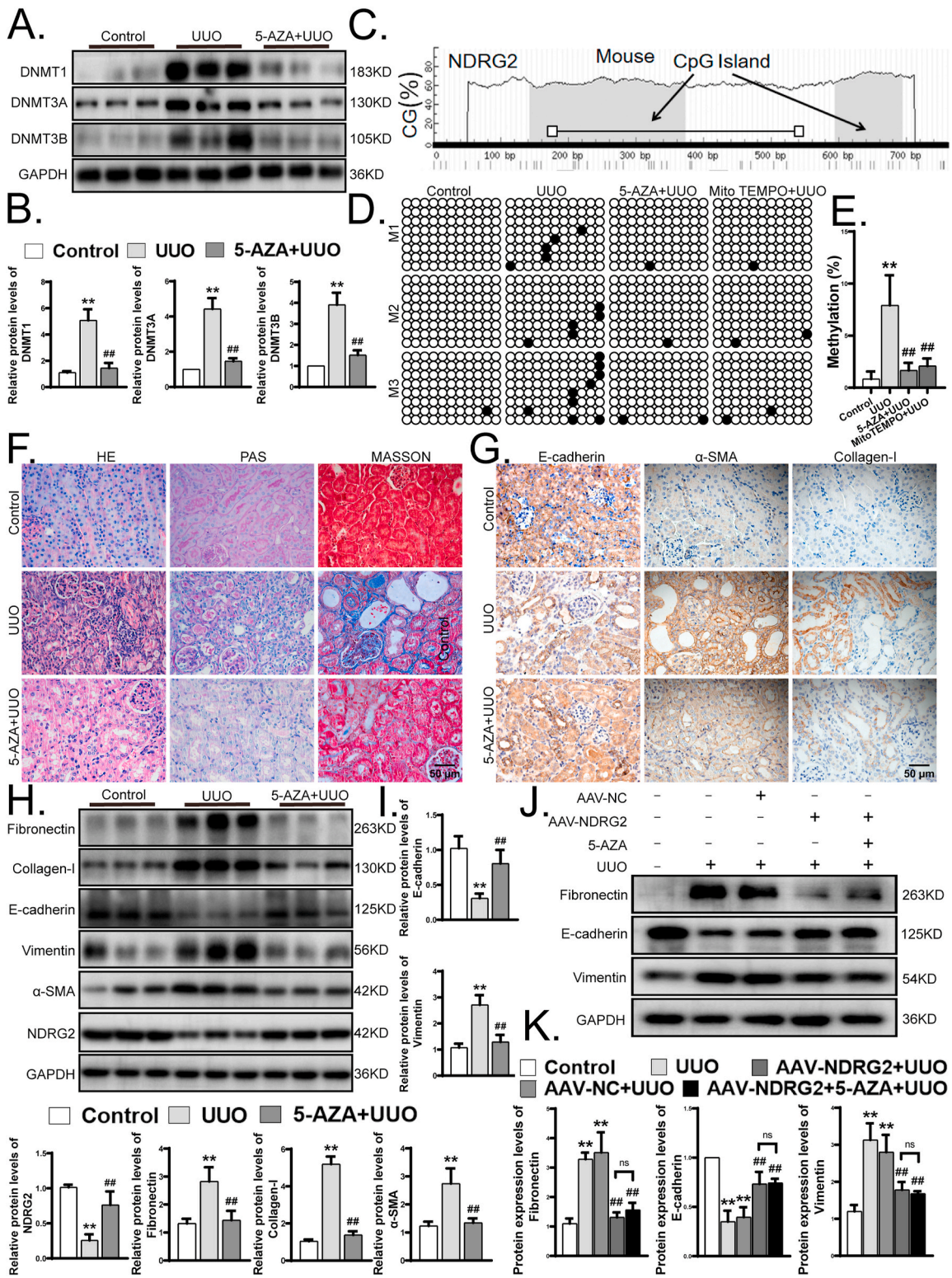

Fig. 5. 5-AZA-dC alleviated NDRG2 promoter hyper-methylation and UUO-associated renal fibrosis. (A) Protein expression levels of DNMT1, DNAM3A and DNMT3B from control, UUO mice, and UUO mice treated with 5-AZA-dC (0.35 mg/kg) day 1 before UUO operation assayed by Western blotting (3 samples from each group). (B) Quantification of (A). (C) Schematic diagram of mouse NDRG2 promoter. The CpG island is in gray. The relative locations of bisulfate-specific PCR (BSP) primers are indicated. (D) BSP assay of experimental mice. Renal tissues from the above-mentioned experimental mice were analyzed by BSP analysis. The black circle represents methylated cytosine and the white circle represents the un-methylated. Results of three mice (M1–M3) from each group and eight clones from each mouse are shown. (E) Quantification of (D). (F) Representative H&E, PAS and Masson's trichrome-stained kidney sections from experimental mice as above. (G) Representative kidney immunohistochemical staining of E-cadherin, Collagen-I, α-SMA from experimental mice as above. (H) Western blotting assay for the protein expression of Fibronectin, Collagen-I, E-cadherin, Vimentin, α-SMA and NDRG2 from experimental mice as above (3 samples from each group). (I) Quantification of (H). (J) Western blotting assay for the protein expression of Fibronectin, E-cadherin, Vimentin from experimental mice as above. (K) Quantification of (J). The statistics were based on at least three independent experiments. $^{**}p < 0.01$ versus control; $^{\#}p < 0.05$, $^{\#\#}p < 0.01$ versus UUO by one-way ANOVA.

demethylation of NDRG2 promoter and then inhibit renal fibrosis in UUO mice.

3.6. Elimination of ROS alleviated hypoxia-induced fibrotic protein expression and NDRG2 repression in HK2 cells

Since ROS play an important role in DNA promoter hyper-methylation [17,35], we speculated that ROS were responsible for NDRG2 promoter hyper-methylation. Firstly, we detected the intracellular ROS levels in HK2 cells under normxia or hypoxia conditions. As mitochondrial ROS are the main source of cellular ROS, Mito SOX Red Mitochondrial Superoxide Indicator (MitoSOX) was used to detected the activity of ROS. Compared to HK2 cells under normxia conditions, HK2 cells exposed to hypoxia exhibited increased fluorescence intensity of MitoSOX (Fig. 6A). To further investigate the effect of ROS in hypoxia-induced fibrotic protein expression in cells, Mito-TEMPO was used to incubate HK-2 cells. HK-2 cells were pretreated with Mito-TEMPO for 2 h and cultured in hypoxic condition for 48 h, while the cells cultured under normoxia served as control. As shown in Fig. 6A, Mito-TEMPO treatment significantly decreased fluorescence intensity of MitoSOX Red, which suggested that Mito-TEMPO treatment markedly rescued the increased mitochondrial ROS stress induced by hypoxia exposure. Then, we examined whether the decrease of mitochondrial ROS was accompanied by the decreased fibrotic protein expression in HK2 cells. We found that Mito-TEMPO treatment restored the expression of NDRG2 and E-cadherin, and mitigated the upregulation of Fibronectin, Vimentin and α-SMA, in hypoxic-induce HK2 cells (Fig. 6B–F). To further determine the effect of Mito-TEMPO in NDRG2-mediated protective effect in hypoxia-induced HK2 cells, we investigated the effects of NDRG2 knockdown on the anti-fibrotic effects of Mito-TEMPO. We found that the anti-fibrotic activities of Mito-TEMPO were largely abolished when NDRG2 was knocked down (Fig. 6G–I). Overall, these results clearly indicated that the regulation of Mito-TEMPO on NDRG2 was the key mechanism of Mito-TEMPO against fibrotic protein expression in HK2 cells under hypoxia conditions.

3.7. Elimination of ROS inhibited hypoxia-induced hyper-methylation of NDRG2 promoter in HK2 cells

Previous studies have shown that ROS are involved in regulating DNA promoter methylation and regulating gene expression at the transcriptional level by regulating the expression level of DNMTS [25]. We found that Mito-TEMPO could alleviate aberrant DNMTS expression (Fig. 7A–F). To further determine whether Mito-TEMPO could inhibit hypoxia-induced aberrant NDRG2 promoter methylation, we performed MSP. The results of MSP revealed that NDRG2 promoter displayed low basal methylation in control group (about 18%), while HK2 cells in hypoxia group exhibited increased methylation up to 65%. However, Mito-TEMPO inhibited such hyper-methylation down to 29% (Fig. 7G and H). In addition, the dual-luciferase reporter gene assay verified that Mito-TEMPO treatment successfully restored hypoxia-induced lower transcription of NDRG2 promoter reporter (Fig. 7I). These results suggested that reducing mitochondrial ROS could reverse the hyper-methylation of NDRG2 promoter. To further verify our hypothesis, ChIP-qPCR was used to analyze whether reducing mitochondrial ROS could decrease the binding force between DNMTS and NDRG2 promoter region in hypoxia-induced HK2 cells. As shown in Fig. 7J, the results of ChIP-qPCR indicated that Mito-TEMPO treatment reduced the increase of binding force between DNMTS and the NDRG2 promoter caused by hypoxia. These findings suggested that NDRG2 expression was Mito-stress-dependently inhibited by up-regulation of DNMTS in hypoxia-treated HK2 cells. Glutathione is known to be an important antioxidant in vivo, widely involved in the maintenance of cellular redox homeostasis [36,37]. To further confirm whether ROS was involved in the regulation of NDRG2 expression by regulating DNMTS expression levels, we pretreated HK2 cells with GSH and its precursors (N-acetyl cysteine, NAC). The results showed that, as with Mito-TEMPO pretreatment, the expression level of DNMT1/3A/3B was significantly decreased in HK2 cells pretreated with GSHee (glutathione ethyl ester) and NAC, while the expression level of NDRG2 was significantly increased (Supplementary Figs. 8A and B). Collectively, these results clearly indicated that ROS were involved in the hypoxia-induced fibrotic protein expression in HK2 cells by regulating the DNA methylation of NDRG2 promoter.

3.8. Inhibition of ROS attenuated NDRG2 promoter hyper-methylation and renal fibrosis in UUO

We further verified whether Mito-TEMPO had the same protective effects in fibrotic kidney of UUO. To investigate the effect of ROS inhibition against renal damage in UUO mouse model, Mito-TEMPO (1 mg/kg) was intraperitoneally injected to mice every other day from day 1 before surgery. The results showed that Mito-TEMPO reversed UUO-associated DNMTS aberrations (figure 8A-C), which suggested that Mito-TEMPO might reduce the DNA methylation level of NDRG2 promoter, thereby restoring the expression of NDRG2. Therefore, we performed BSP assay on mouse kidneys, and the results showed that the methylation level of NDRG2 promoter in UUO kidney increased from $0.83 \pm 0.72\%$ to $7.92 \pm 2.89\%$ ($P < 0.01$), and Mito-TEMPO treatment reduced the methylation level to $2.083 \pm 0.72\%$ ($P < 0.01$, Fig. 5D–E). In addition, following UUO, Mito-TEMPO treated mice showed less histopathological and structural damage and collagen deposition than UUO mice (Fig. 8D). Furthermore, our results also showed that Mito-TEMPO mitigated abnormal expression of NDRG2 and fibrosis-related proteins induced by UUO (Fig. 8E–H). Together, these findings demonstrated that inhibition of ROS could restore the expression of NDRG2 by suppressing UUO-induced DNMTS aberrations which were in line with the in vitro experiment.

4. Discussion

NDRG2 is known as an important tumor suppressor gene, and its role in fibrotic diseases has been gradually explored in recent years. With the extensive research on renal fibrosis, DNA methylation modification of susceptibility genes to renal fibrosis is becoming a new role in this process [14,15]. In this study, we investigated early upstream events of epigenetic induction of NDRG2 inhibition and their role in renal fibrosis. Some significant findings were made in this study, which contribute to a better understanding of the DNA-epigenetic regulation of the expression of NDRG2 in renal fibrosis and its regulatory mechanisms: (1) Our study was the first to verify the anti-fibrotic effect of NDRG2 in renal fibrosis in vivo and in vitro; (2) In the development of renal fibrosis, the elevations of DNMT1/3A/3B led to hyper-methylation of NDRG2 promoter, resulting in transcriptional inhibition and decreased expression of NDRG2; (3) We found that in the development of renal fibrosis, excessive ROS was an important risk factor leading to increased activity of DNA methyltransferases. Mitochondria-targeted antioxidants effectively reduced hyper-methylation of NDRG2 promoter, restored NDRG2 expression level and inhibited renal fibrosis; (4) In HK2 cells with NDRG2 knockdown, the anti-fibrotic effects of both methyltransferase inhibitors and mitochondria-targeted antioxidants were eliminated. Thus, our study demonstrated that aberrant DNMT1/3A/3B elevations and the resultant suppressions of NDRG2 contribute to renal fibrosis, revealing a new signaling pathway linking ROS and DNA methylation with NDRG2 deficiency and renal fibrosis.

Abundant evidence suggests that NDRG2 is extensively involved in important cellular processes and plays an important role in diseases such as tumor, fibrosis and inflammation by regulating multiple signaling pathways [4,5,38]. For example, previous studies have reported that NDRG2 could reduce liver fibrosis and improve liver function, preventing phosphorylation of ERK and Smad3 [5,39]. Hu et al. found that NDRG2 was significantly expressed during the differentiation of renal

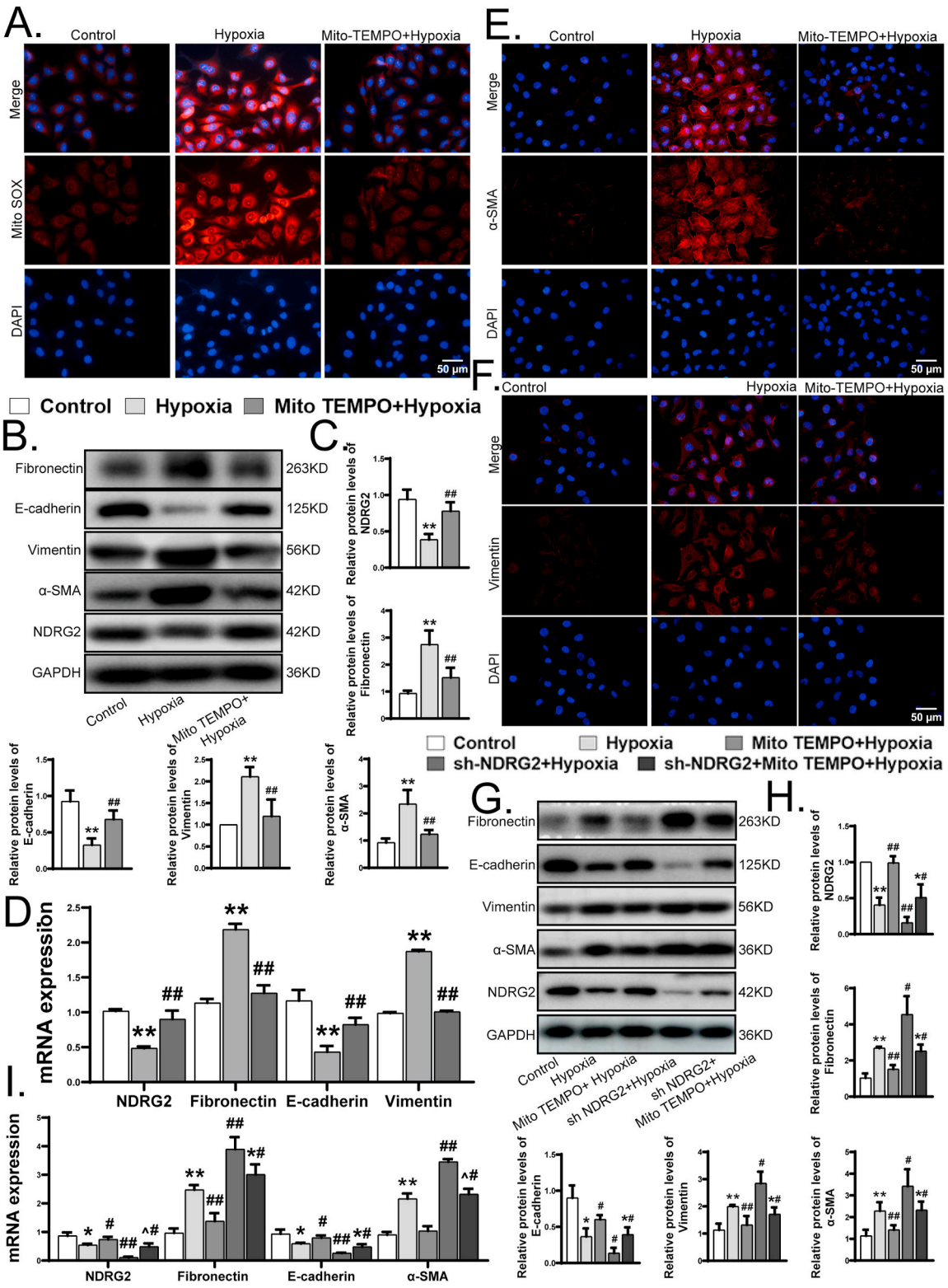

Fig. 6. Elimination of ROS alleviated hypoxia-induced fibrotic protein expression and NDRG2 repression in HK2 cells. (A) ROS expression level of HK2 cells pre-treated with Mito-TEMPO for 2 h and cultured in normxia or hypoxia conditions for 48h assessed by MitoSOX assay. (B) Western blotting assay for the protein expression of NDRG2, Fibronectin, E-cadherin, Vimentin and α-SMA. (C) Quantification of (B). (D) Real-time PCR analysis in HK2 cells. (E, F) Representative immunofluorescence images of Vimentin and α-SMA. (G) Western blotting assay in HK2 cells transfected with NDRG2 shRNA or Scramble shRNA cultured in hypoxia or normoxia for 48 h with or without Mito-TEMPO. (H) Quantification of (G). (I) Real-time PCR analysis in HK2 cells. The statistics were based on at least three independent experiments. *$p < 0.05$, **$p < 0.01$ versus control; $^{\#}p < 0.05$, $^{\#\#}p < 0.01$ versus hypoxia; $^{\wedge\#}p < 0.05$, $^{*\#}p < 0.01$ versus shNDRG2+hypoxia by one-way ANOVA.

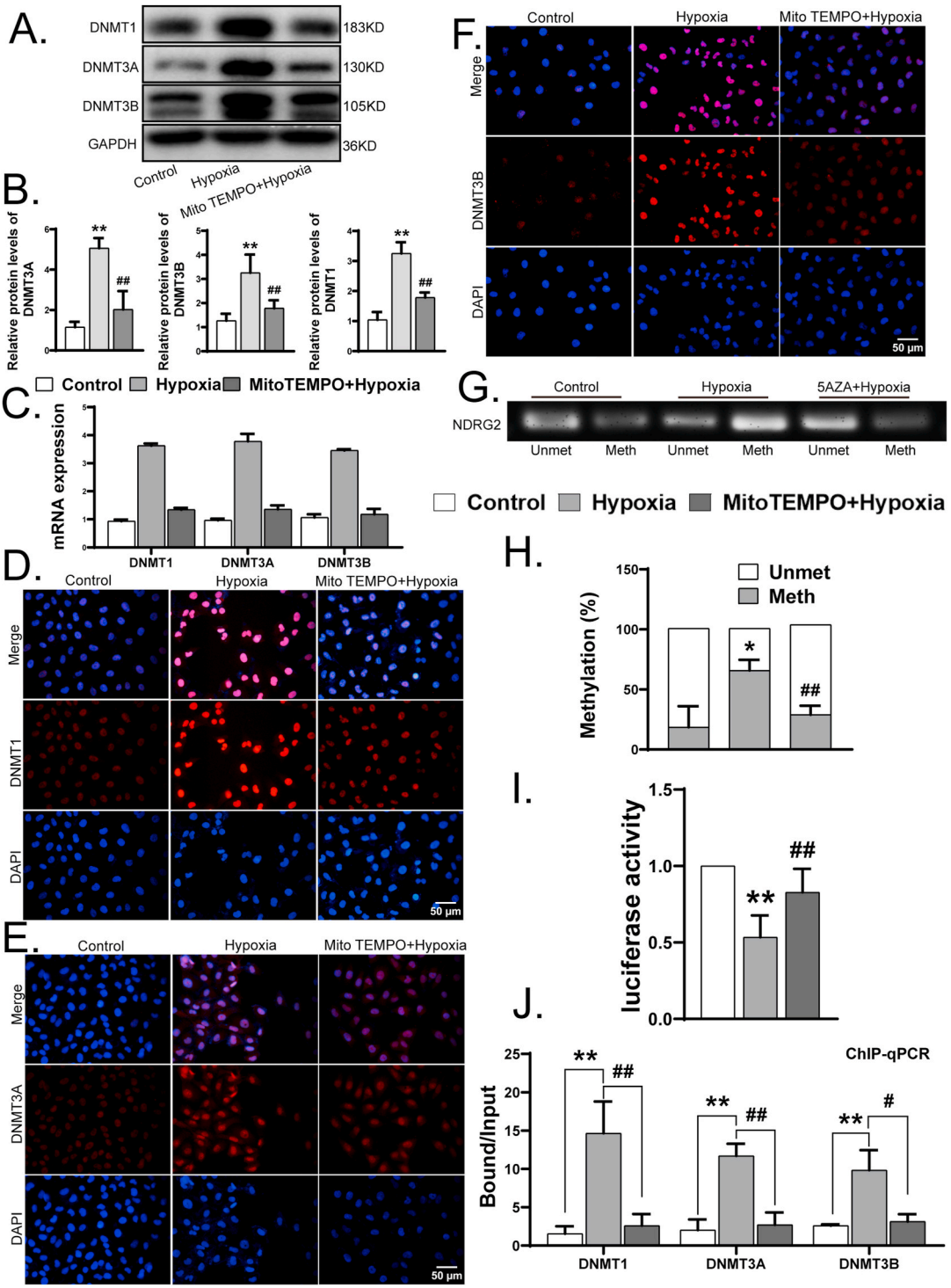

Fig. 7. Elimination of ROS inhibited hypoxia-induced hyper-methylation of NDRG2 promoter in HK2 cells. (A) Western blotting assay for the expression of DNMT1, DNMT3A and DNMT3B in HK2 cells pretreated with Mito-TEMPO for 2 h and cultured in normxia or hypoxia conditions for the following 48h. (B) Quantification of (A). (C) Real-time PCR analysis. (D–F) Representative immunofluorescence images of DNMT1, DNMT3A, and DNMT3B in HK2 cells. (G) MSP analysis of NDRG2 promoter methylation in HK2 cells. (H) Quantifications for (G). (I) Luciferase assay. A Human NDRG2 promoter reporter plasmid plus a renilla luciferase control were co-transfected into HK2 cells and the cells were cultured in normxia or hypoxia conditions in presence or absence of Mito-TEMPO for the following 48h. The cell lysates were assayed for luciferase activities, which were normalized with renilla activities. (J) ChIP-qPCR performed using primer sets specific for NDRG2 promoter. ChIP products using antibodies against DNMT1, DNMT3A, and DNMT3B were analyzed by qPCR. The statistics were based on at least three independent experiments. *$p < 0.05$, **$p < 0.01$ versus control, #$p < 0.05$, ##$p < 0.01$ versus hypoxia by one-way ANOVA.

tubular epithelial cells [40]. In addition, NDRG2 expression was decreased in HK-2 cells induced by TGF-β1 and NDRG2 knockdown promoted EMT process and ECM production, leading to renal fibrosis [6]. These studies suggest that NDRG2 may play an important role in kidney fibrosis. In this study, we found that the expression level of NDRG2 was significantly reduced in both fibrotic kidneys and hypoxic-treated HK2 cells, which greatly stimulated our interest in further exploring the role of NDRG2 in the progression of renal fibrosis.

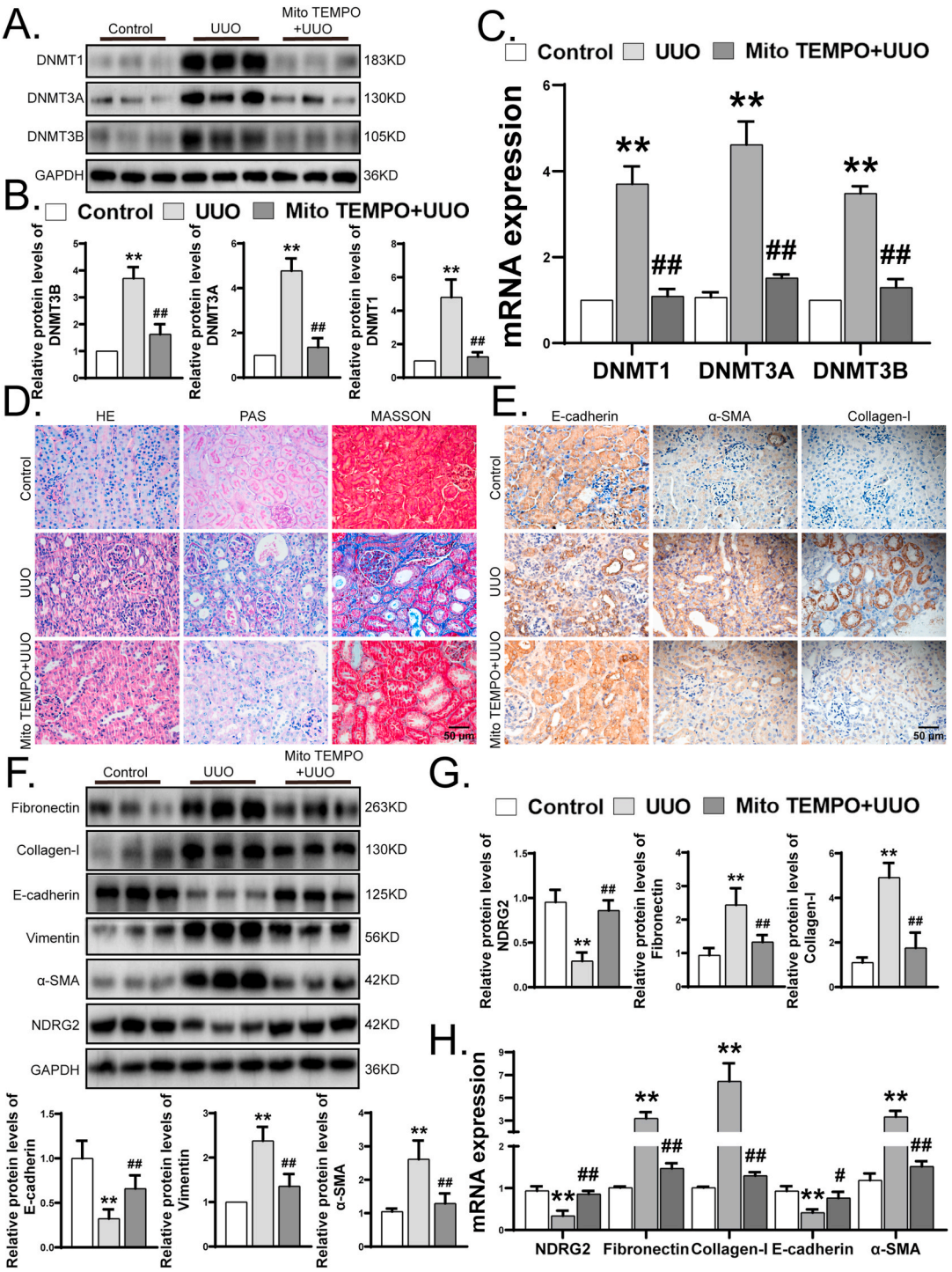

Fig. 8. Inhibition of ROS attenuated NDRG2 promoter hyper-methylation and renal fibrosis in UUO. (A) Protein expression levels of DNMT1, DNAM3A and DNMT3B from control, UUO mice, and UUO mice treated with Mito-TEMPO (1 mg/kg) day 1 before UUO operation assayed by Western blotting (3 samples from each group). (B) Quantification of (A). (C) Real-time PCR analysis. (D) Representative H&E, PAS and Masson's trichrome-stained kidney sections from experimental mice as above. (E) Representative renal immunohistochemical staining of E-cadherin, α-SMA and Collagen-I from experimental mice as above. (F) Western blotting assay for the protein expression of Fibronectin, Collagen-I, E-cadherin, Vimentin, α-SMA and NDRG2 from experimental mice as above (3 samples from each group). (G) Quantification of (F). (H) Gene expression levels of NDRG2, Fibronectin, Collagen-I, E-cadherin, α-SMA assayed by Real-time PCR. The statistics were based on at least three independent experiments. *$p < 0.05$, **$p < 0.01$ versus control; $^{\#}p < 0.05$, $^{\#\#}p < 0.01$ versus UUO by one-way ANOVA.

Furthermore, NDRG2 overexpression alleviated renal fibrosis of UUO mice and hypoxia-induced HK2 cell fibrotic response, supporting our hypothesis that NDRG2 mediated an anti-fibrotic role in renal fibrosis. We believe that the anti-fibrotic effect of over-expression of NDRG2 in vivo is the result of the combined action of various cells and molecules. However, our in vitro study only explored the role of fibrotic response of HK2 cell in the process of renal fibrosis. Our subsequent studies will explore which cell types and the specific regulatory networks are involved in the anti-fibrotic effect of NDRG2 in complex organism environments.

DNA methylation is the most common epigenetic modification and a major regulator of the activity of transcriptional [41,42], associated

with silencing of gene expression [43]. Previous studies have shown that abnormal DNA methylation is associated with the development of a variety of human diseases [44–46]. In fact, there is increasing evidence that DNA methylation of multiple genes associated with renal fibrosis is involved in the pathogenesis of renal fibrosis and promotes the progression of CKD [27,28,47]. In addition, results from a cohort study of chronic kidney disease showed that the level of global DNA methylation was positively associated with loss of renal function in patients diagnosed with CKD [10]. The NDRG2 promoter contains evolutionarily conserved CpG islands, which are hyper-methylated in primary tumors [48,49], and are closely related to the loss of NDRG2 expression in liver cancer [50]. In addition, deletion of NDRG2 expression has been reported to be associated with promoter hyper-methylation in liver fibrosis [51]. DNMTS are key enzyme regulating DNA methylation [9,52], and the epigenetic inactivation of key genes mediated by DNMTS are closely related to the development and progression of renal fibrosis [14,53,54]. We also found that methyltransferase inhibitor 5AZA-dC reversed NDRG2 loss in a DNMT1/3A/3B-dependent manner, thereby alleviated hypoxia-induced fibrotic response in HK2 cells and UUO-induced renal fibrosis.

A growing number of studies have shown the presence of chronic renal hypoxia [55,56] in patients with CKD and in mouse models associated with CKD, which is a common pathway to end-stage renal failure [57,58]. In addition, ROS induced by chronic hypoxia have been widely confirmed to play an important role in renal injury from various causes [19], but the molecular mechanism of ROS mediating renal fibrosis has not been elucidated. In this study, we found that ROS levels in hypoxia-treated HK2 cells were significantly increased, and inhibition of ROS effectively alleviated HK2 cell fibrotic response induced by hypoxia and renal fibrosis induced by UUO. Previous studies have shown that chronic hypoxia and its resulting oxidative stress significantly increased global DNA methylation in cardiac fibroblasts, and inhibition of oxidative stress reduced myocardial fibrosis induced by hypoxia [59]. In addition, ROS can increase the expression level of methyltransferase, which is the main cause of abnormal DNA methylation of the target gene in renal fibrosis [26–28]. More importantly, our study showed that treatment of Mito-TEMPO increased NDRG2 expression in hypoxia-induced HK2 cells and fibrotic kidneys of UUO mice. Based on the above evidence, we hypothesized that oxidative stress induced by hypoxia was an upstream event that induced methylation of the NDRG2 promoter. Further studies showed that Mito-TEMPO effectively reversed the epigenetic alterations and reduced the renal fibrosis alterations in a NDRG2 dependent manner. Interestingly, the anti-fibrotic effect of Mito-TEMPO was eliminated in HK2 cells with NDRG2 knockdown. These results confirmed our hypothesis that ROS was involved in renal fibrosis by enhancing the activity of DNA methyltransferases, which led to DNA methylation and NDRG2 inhibition.

Taken together, the results of this study confirmed the critical anti-fibrosis role of NDRG2 in renal fibrosis. Moreover, ROS promoted hyper-methylation of NDRG2 promoter in a DNMT-dependent manner and was involved in DNA methylation regulation of the expression of NDRG2 in renal fibrosis. This study not only reveals the unique mechanism of renal fibrosis, but also provides new ideas for future treatment of CKD.

Availability of data and materials

The datasets analyzed during the current study are temporarily unpublished for research reasons, but are available from the respective authors upon reasonable request.

Declaration of competing interest

The authors state that they have nothing to disclose and declare no conflict of interest.

Data availability

The datasets analyzed during the current study are temporarily unpublished for research reasons, but are available from the respective authors upon reasonable request.

Acknowledgments

This work was funded by National Natural Science Foundation of China (Grant: 81873615, 82070744, 81770723, 81400732), Academic promotion programme of Shandong First Medical University (NO: 2019QL022) and Taishan Scholars Program (NO: ts201712090, tsqn201812138).

Appendix A. Supplementary data

Supplementary data to this article can be found online at https://doi.org/10.1016/j.redox.2023.102674.

References

[1] M. Stern-Zimmer, R. Calderon-Margalit, K. Skorecki, A. Vivante, Childhood risk factors for adulthood chronic kidney disease, Pediatr. Nephrol. 36 (6) (2021) 1387–1396.
[2] B.D. Humphreys, Mechanisms of renal fibrosis, Annu. Rev. Physiol. 80 (2018) 309–326.
[3] S.L. Lin, Y.M. Chen, W.C. Chiang, T.J. Tsai, W.Y. Chen, Pentoxifylline: a potential therapy for chronic kidney disease, Nephrology 9 (4) (2004) 198–204.
[4] M. Ding, X. Bu, Z. Li, H. Xu, L. Feng, J. Hu, et al., NDRG2 ablation reprograms metastatic cancer cells towards glutamine dependence via the induction of ASCT2, Int. J. Biol. Sci. 16 (16) (2020) 3100–3115.
[5] J. Yang, J. Zheng, L. Wu, M. Shi, H. Zhang, X. Wang, et al., NDRG2 ameliorates hepatic fibrosis by inhibiting the TGF-β1/Smad pathway and altering the MMP2/TIMP2 ratio in rats, PLoS One 6 (11) (2011), e27710.
[6] Z. Jin, C. Gu, F. Tian, Z. Jia, J. Yang, NDRG2 knockdown promotes fibrosis in renal tubular epithelial cells through TGF-β1/Smad3 pathway, Cell Tissue Res. 369 (3) (2017) 603–610.
[7] F. Ge, P. Zhang, J. Niu, X. Pei, C. Lian, R. Yu, et al., NDRG2 and TLR7 as novel DNA methylation prognostic signatures for acute myelocytic leukemia, J. Cell. Physiol. 235 (4) (2020) 3790–3797.
[8] J. Gödeke, E. Luxenburger, F. Trippel, K. Becker, B. Häberle, J. Müller-Höcker, et al., Low expression of N-myc downstream-regulated gene 2 (NDRG2) correlates with poor prognosis in hepatoblastoma, Hepatology international 10 (2) (2016) 370–376.
[9] F.I. Daniel, K. Cherubini, L.S. Yurgel, M.A. de Figueiredo, F.G. Salum, The role of epigenetic transcription repression and DNA methyltransferases in cancer, Cancer 117 (4) (2011) 677–687.
[10] M.R. Wing, J.M. Devaney, M.M. Joffe, D. Xie, H.I. Feldman, E.A. Dominic, et al., DNA methylation profile associated with rapid decline in kidney function: findings from the CRIC study, Nephrol. Dial. Transplant. : official publication of the European Dialysis and Transplant Association - European Renal Association 29 (4) (2014) 864–872.
[11] G.H. Rauscher, J.K. Kresovich, M. Poulin, L. Yan, V. Macias, A.M. Mahmoud, et al., Exploring DNA methylation changes in promoter, intragenic, and intergenic regions as early and late events in breast cancer formation, BMC Cancer 15 (2015) 816.
[12] M. Møller, S.H. Strand, K. Mundbjerg, G. Liang, I. Gill, C. Haldrup, et al., Heterogeneous patterns of DNA methylation-based field effects in histologically normal prostate tissue from cancer patients, Sci. Rep. 7 (2017), 40636.
[13] Q. Zhang, S. Yin, L. Liu, Z. Liu, W. Cao, Rhein reversal of DNA hypermethylation-associated Klotho suppression ameliorates renal fibrosis in mice, Sci. Rep. 6 (2016), 34597.
[14] S. Yin, Q. Zhang, J. Yang, W. Lin, Y. Li, F. Chen, et al., TGFβ-incurred epigenetic aberrations of miRNA and DNA methyltransferase suppress Klotho and potentiate renal fibrosis, Biochim. Biophys. Acta Mol. Cell Res. 1864 (7) (2017) 1207–1216.
[15] W. Bechtel, S. McGoohan, E.M. Zeisberg, G.A. Müller, H. Kalbacher, D.J. Salant, et al., Methylation determines fibroblast activation and fibrogenesis in the kidney, Nat. Med. 16 (5) (2010) 544–550.
[16] D. Ziech, R. Franco, A. Pappa, M.I. Panayiotidis, Reactive oxygen species (ROS)–induced genetic and epigenetic alterations in human carcinogenesis, Mutat. Res. 711 (1–2) (2011) 167–173.
[17] S.O. Lim, J.M. Gu, M.S. Kim, H.S. Kim, Y.N. Park, C.K. Park, et al., Epigenetic changes induced by reactive oxygen species in hepatocellular carcinoma: methylation of the E-cadherin promoter, Gastroenterology 135 (6) (2008) 2128–2140, 40.e1-2140.
[18] A.C. Campos, F. Molognoni, F.H. Melo, L.C. Galdieri, C.R. Carneiro, V. D'Almeida, et al., Oxidative stress modulates DNA methylation during melanocyte anchorage blockade associated with malignant transformation, Neoplasia 9 (12) (2007) 1111–1121.

[19] N.R. Prabhakar, G.K. Kumar, J. Nanduri, G.L. Semenza, ROS signaling in systemic and cellular responses to chronic intermittent hypoxia, Antioxidants Redox Signal. 9 (9) (2007) 1397–1403.
[20] L.M. Sandalio, M. Rodríguez-Serrano, M.C. Romero-Puertas, L.A. del Río, Role of peroxisomes as a source of reactive oxygen species (ROS) signaling molecules, Subcell. biochem. 69 (2013) 231–255.
[21] A. Duni, V. Liakopoulos, S. Roumeliotis, D. Peschos, E. Dounousi, Oxidative stress in the pathogenesis and evolution of chronic kidney disease: untangling ariadne's thread, Int. J. Mol. Sci. 20 (15) (2019).
[22] M.V. Irazabal, V.E. Torres, Reactive oxygen species and redox signaling in chronic kidney disease, Cells 9 (6) (2020).
[23] C. Li, N. Xie, Y. Li, C. Liu, F.F. Hou, J. Wang, N-acetylcysteine ameliorates cisplatin-induced renal senescence and renal interstitial fibrosis through sirtuin1 activation and p53 deacetylation, Free Radical Biol. Med. 130 (2019) 512–527.
[24] T. He, J. Xiong, L. Nie, Y. Yu, X. Guan, X. Xu, et al., Resveratrol inhibits renal interstitial fibrosis in diabetic nephropathy by regulating AMPK/NOX4/ROS pathway, J. Mol. Med. 94 (12) (2016) 1359–1371.
[25] Q. Wu, X. Ni, ROS-mediated DNA methylation pattern alterations in carcinogenesis, Curr. Drug Targets 16 (1) (2015) 13–19.
[26] C.Y. Sun, S.C. Chang, M.S. Wu, Suppression of Klotho expression by protein-bound uremic toxins is associated with increased DNA methyltransferase expression and DNA hypermethylation, Kidney Int. 81 (7) (2012) 640–650.
[27] Q. Yang, H.Y. Chen, J.N. Wang, H.Q. Han, L. Jiang, W.F. Wu, et al., Alcohol promotes renal fibrosis by activating Nox2/4-mediated DNA methylation of Smad7, Clin. Sci. 134 (2) (2020) 103–122 (London, England : 1979).
[28] Y. Yu, X. Guan, L. Nie, Y. Liu, T. He, J. Xiong, et al., DNA hypermethylation of sFRP5 contributes to indoxyl sulfate-induced renal fibrosis, J. Mol. Med. 95 (6) (2017) 601–613.
[29] T. Qin, R. Du, F. Huang, S. Yin, J. Yang, S. Qin, et al., Sinomenine activation of Nrf2 signaling prevents hyperactive inflammation and kidney injury in a mouse model of obstructive nephropathy, Free Radical Biol. Med. 92 (2016) 90–99.
[30] Y. Ma, F. Cai, X. Huang, H. Wang, B. Yu, J. Wang, et al., Mannose-binding lectin activates the nuclear factor-κB and renal inflammation in the progression of diabetic nephropathy, Faseb. J. : official publication of the Federation of American Societies for Experimental Biology 36 (3) (2022), e22227.
[31] B. Wang, J. Wang, W. He, Y. Zhao, A. Zhang, Y. Liu, et al., Exogenous miR-29a attenuates muscle atrophy and kidney fibrosis in unilateral ureteral obstruction mice, Hum. Gene Ther. 31 (5–6) (2020) 367–375.
[32] J. Zhang, L. Cao, X. Wang, Q. Li, M. Zhang, C. Cheng, et al., The E3 ubiquitin ligase TRIM31 plays a critical role in hypertensive nephropathy by promoting proteasomal degradation of MAP3K7 in the TGF-β1 signaling pathway, Cell Death Differ. 29 (3) (2022) 556–567.
[33] M. Tepel, P. Roerig, M. Wolter, D.H. Gutmann, A. Perry, G. Reifenberger, et al., Frequent promoter hypermethylation and transcriptional downregulation of the NDRG2 gene at 14q11.2 in primary glioblastoma, Int. J. Cancer 123 (9) (2008) 2080–2086.
[34] L. Shen, X. Qu, Y. Ma, J. Zheng, D. Chu, B. Liu, et al., Tumor suppressor NDRG2 tips the balance of oncogenic TGF-β via EMT inhibition in colorectal cancer, Oncogenesis 3 (2) (2014) e86.
[35] H. Xie, P. Chen, H.W. Huang, L.P. Liu, F. Zhao, Reactive oxygen species downregulate ARID1A expression via its promoter methylation during the pathogenesis of endometriosis, Eur. Rev. Med. Pharmacol. Sci. 21 (20) (2017) 4509–4515.
[36] C.C. Franklin, D.S. Backos, I. Mohar, C.C. White, H.J. Forman, T.J. Kavanagh, Structure, function, and post-translational regulation of the catalytic and modifier subunits of glutamate cysteine ligase, Mol. Aspect. Med. 30 (1–2) (2009) 86–98.
[37] R. Parsanathan, S.K. Jain, Glutathione deficiency induces epigenetic alterations of vitamin D metabolism genes in the livers of high-fat diet-fed obese mice, Sci. Rep. 9 (1) (2019), 14784.
[38] X. Li, X. Wu, P. Luo, L. Xiong, Astrocyte-specific NDRG2 gene: functions in the brain and neurological diseases, Cell. Mol. Life Sci. : CM 77 (13) (2020) 2461–2472.
[39] H. Huang, K. Wang, Q. Liu, F. Ji, H. Zhou, S. Fang, et al., The active constituent from gynostemma pentaphyllum prevents liver fibrosis through regulation of the TGF-β1/NDRG2/MAPK Axis, Front. Genet. 11 (2020), 594824.
[40] X.L. Hu, X.P. Liu, Y.C. Deng, S.X. Lin, L. Wu, J. Zhang, et al., Expression analysis of the NDRG2 gene in mouse embryonic and adult tissues, Cell Tissue Res. 325 (1) (2006) 67–76.
[41] K. Skvortsova, C. Stirzaker, P. Taberlay, The DNA methylation landscape in cancer, Essays Biochem. 63 (6) (2019) 797–811.
[42] M. Wątroba, I. Dudek, M. Skoda, A. Stangret, P. Rzodkiewicz, D. Szukiewicz, Sirtuins, epigenetics and longevity, Ageing Res. Rev. 40 (2017) 11–19.
[43] P.A. Jones, D. Takai, The role of DNA methylation in mammalian epigenetics, Science 293 (5532) (2001) 1068–1070.
[44] H.T. Bjornsson, M.D. Fallin, A.P. Feinberg, An integrated epigenetic and genetic approach to common human disease, Trends Genet. : TIG (Trends Genet.) 20 (8) (2004) 350–358.
[45] A. Portela, M. Esteller, Epigenetic modifications and human disease, Nat. Biotechnol. 28 (10) (2010) 1057–1068.
[46] G. Egger, G. Liang, A. Aparicio, P.A. Jones, Epigenetics in human disease and prospects for epigenetic therapy, Nature 429 (6990) (2004) 457–463.
[47] Y. Li, F. Chen, A. Wei, F. Bi, X. Zhu, S. Yin, et al., Klotho recovery by genistein via promoter histone acetylation and DNA demethylation mitigates renal fibrosis in mice, J. Mol. Med. 97 (4) (2019) 541–552.
[48] P. Vaitkiene, I. Valiulyte, B. Glebauskiene, R. Liutkeviciene, N-myc downstream-regulated gene 2 (NDRG2) promoter methylation and expression in pituitary adenoma, Diagn. Pathol. 12 (1) (2017) 33.
[49] X. Chang, Z. Li, J. Ma, P. Deng, S. Zhang, Y. Zhi, et al., DNA methylation of NDRG2 in gastric cancer and its clinical significance, Dig. Dis. Sci. 58 (3) (2013) 715–723.
[50] D.C. Lee, Y.K. Kang, W.H. Kim, Y.J. Jang, D.J. Kim, I.Y. Park, et al., Functional and clinical evidence for NDRG2 as a candidate suppressor of liver cancer metastasis, Cancer Res. 68 (11) (2008) 4210–4220.
[51] X.Y. Liu, Y.C. Fan, S. Gao, J. Zhao, F. Li, J. Zhang, et al., Hypermethylation of the N-myc downstream-regulated gene 2 promoter in peripheral Blood mononuclear cells is associated with liver fibrosis in chronic hepatitis B, Tohoku J. Exp. Med. 241 (2) (2017) 155–163.
[52] Z. Chen, Y. Zhang, Role of mammalian DNA methyltransferases in development, Annu. Rev. Biochem. 89 (2020) 135–158.
[53] S. Pushpakumar, S. Kundu, N. Narayanan, U. Sen, DNA hypermethylation in hyperhomocysteinemia contributes to abnormal extracellular matrix metabolism in the kidney, Faseb. J. : official publication of the Federation of American Societies for Experimental Biology 29 (11) (2015) 4713–4725.
[54] P. Gondaliya, A. Dasare, A. Srivastava, K. Kalia, miR29b regulates aberrant methylation in In-Vitro diabetic nephropathy model of renal proximal tubular cells, PLoS One 13 (11) (2018), e0208044.
[55] L.G. Fine, J.T. Norman, Chronic hypoxia as a mechanism of progression of chronic kidney diseases: from hypothesis to novel therapeutics, Kidney Int. 74 (7) (2008) 867–872.
[56] M. Liu, X. Ning, R. Li, Z. Yang, X. Yang, S. Sun, et al., Signalling pathways involved in hypoxia-induced renal fibrosis, J. Cell Mol. Med. 21 (7) (2017) 1248–1259.
[57] I. Mimura, M. Nangaku, The suffocating kidney: tubulointerstitial hypoxia in end-stage renal disease, Nat. Rev. Nephrol. 6 (11) (2010) 667–678.
[58] M. Nangaku, Chronic hypoxia and tubulointerstitial injury: a final common pathway to end-stage renal failure, J. Am. Soc. Nephrol. : JASN (J. Am. Soc. Nephrol.) 17 (1) (2006) 17–25.
[59] A. Rajgarhia, K.R. Ayasolla, N. Zaghloul, J.M. Lopez Da Re, E.J. Miller, M. Ahmed, Extracellular superoxide dismutase (EC-SOD) regulates gene methylation and cardiac fibrosis during chronic hypoxic stress, Front. cardiovasc. med. 8 (2021), 669975.